Bending and vibration of laminated plates by a layerwise meshless formulation.

Publisher copyright

(Article begins on next page)

03 August 2020

Bending and vibration of laminated plates by a layerwise formulation and collocation with radial basis functions

A. J. M. Ferreira [a], C. M. C. Roque [b], E. Carrera [c], M. Cinefra [c], O. Polit [d],

[a]*Departamento de Engenharia Mecânica, Faculdade de Engenharia, Universidade do Porto, Rua Dr. Roberto Frias, 4200-465 Porto, Portugal*

[b]*INEGI, Faculdade de Engenharia, Universidade do Porto, Rua Dr. Roberto Frias, 4200-465 Porto, Portugal*

[c]*Departament of Aeronautics and Aerospace Engineering, Politecnico di Torino, Corso Duca degli Abruzzi, 24, 10129 Torino, Italy*

[d]*Université Paris Ouest - Nanterre, 50 rue de Sevres, 92410 Ville d'Avray, France*

Abstract

This paper addresses the static deformations and free vibration analysis of laminated composite and sandwich plates by collocation with radial basis functions, according to a Layerwise formulation. The present layerwise approach accounts for through-the-thickness deformations. The equations of motion and the boundary conditions are obtained by the Carrera's Unified Formulation, and further interpolated by collocation with radial basis functions.

1 Introduction

The material properties of layered or sandwich composites introduce strong discontinuities of the deformed pseudo-normal to the middle surface at the interfaces, see Fig. 1.

This zig-zag (ZZ) effect i(see an historical review on zig-zag theories by Carrera [1]), makes difficult the use of classical theories such as Kirchhoff [2] or Reissner-Mindlin [3,4] type theories, due to the fact that all layers share the same degrees-of-freedom.

In recent years, radial basis functions (RBFs) proved to be an accurate technique for interpolating data and functions. A radial basis function, $\phi(\|x -$
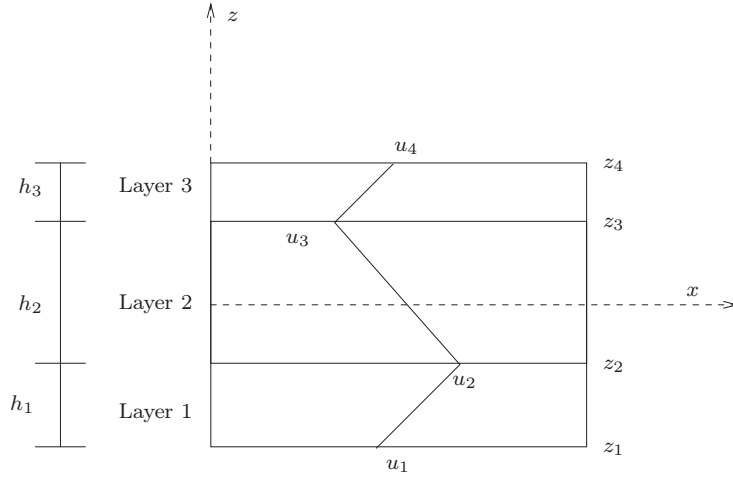
Fig. 1. Scheme of the layerwise assumptions for a three-layered laminate

$x_j\|$) depends on the Euclidian distance between distinct data centers $x_j, j = 1, 2, ..., N \in \mathbb{R}^n$, also called collocation points. Kansa [5] introduced the concept of solving PDEs by an unsymmetric RBF collocation method based upon the MQ interpolation functions. The use of alternative methods to the Finite Element Methods for the analysis of plates, such as the meshless methods based on radial basis functions is atractive due to the absence of a mesh and the ease of collocation methods. The authors have recently applied the RBF collocation to the static deformations of composite beams and plates [6–8].

In this paper it is investigated for the first time how the Unified Formulation can be combined with radial basis functions to the analysis of thick laminated plates, using a layerwise formulation, allowing for through-the-thickness deformations. The quality of the present method in predicting static deformations and free vibrations of thin and thick laminated and sandwich plates is compared and discussed with other methods in some numerical examples.

2 The Unified Formulation for the Layerwise theory

The Unified Formulation (UF) proposed by Carrera [9,10], also known as CUF, has been applied in several finite element analysis, either using the Principle of Virtual Displacements, or by using the Reissner's Mixed Variational theorem. The stiffness matrix components, the external force terms or the inertia terms can be obtained directly with this UF, irrespective of the shear deformation theory being considered.

For the sake of completeness, the Carrera's Unified formulation [9,10] is briefly reviewed. It is shown how to obtain the fundamental nuclei, which allows the derivation of the equations of motion and boundary conditions, for the present

2

RBF collocation.

2.1 Governing equations and boundary conditions in the framework of Unified Formulation

A multi-layered plate with N_l layers is considered. The Principle of Virtual Displacements (PVD) for the mechanical case is defined as:

$$\sum_{k=1}^{N_l} \int_{\Omega_k} \int_{A_k} \left\{ \delta\epsilon_{pG}^k{}^T \sigma_{pC}^k + \delta\epsilon_{nG}^k{}^T \sigma_{nC}^k \right\} d\Omega_k dz = \sum_{k=1}^{N_l} \delta L_e^k \tag{1}$$

where Ω_k and A_k are the integration domains in plane (x,y) and z direction, respectively. Here, k indicates the layer and T the transpose of a vector, and δL_e^k is the external work for the kth layer. G means geometrical relations and C constitutive equations.

Stresses and strains are separated into in-plane and normal components, denoted respectively by the subscripts p and n. The mechanical strains in the kth layer can be related to the displacement field $\mathbf{u}^k = \{u_x^k, u_y^k, u_z^k\}$ via the geometrical relations:

$$\begin{aligned}
\epsilon_{pG}^k &= [\epsilon_{xx}, \epsilon_{yy}, \gamma_{xy}]^{kT} = \mathbf{D}_p^k \mathbf{u}^k \ , \\
\epsilon_{nG}^k &= [\gamma_{xz}, \gamma_{yz}, \epsilon_{zz}]^{kT} = \left(\mathbf{D}_{np}^k + \mathbf{D}_{nz}^k \right) \mathbf{u}^k \ ,
\end{aligned} \tag{2}$$

wherein the differential operator arrays are defined as follows:

$$\mathbf{D}_p^k = \begin{bmatrix} \partial_x & 0 & 0 \\ 0 & \partial_y & 0 \\ \partial_y & \partial_x & 0 \end{bmatrix} , \quad \mathbf{D}_{np}^k = \begin{bmatrix} 0 & 0 & \partial_x \\ 0 & 0 & \partial_y \\ 0 & 0 & 0 \end{bmatrix} , \quad \mathbf{D}_{nz}^k = \begin{bmatrix} \partial_z & 0 & 0 \\ 0 & \partial_z & 0 \\ 0 & 0 & \partial_z \end{bmatrix} , \tag{3}$$

The 3D constitutive equations are given as:

$$\begin{aligned}
\sigma_{pC}^k &= \mathbf{C}_{pp}^k \, \epsilon_{pG}^k + \mathbf{C}_{pn}^k \, \epsilon_{nG}^k \\
\sigma_{nC}^k &= \mathbf{C}_{np}^k \, \epsilon_{pG}^k + \mathbf{C}_{nn}^k \, \epsilon_{nG}^k
\end{aligned} \tag{4}$$

3

with

$$\mathbf{C}_{pp}^k = \begin{bmatrix} C_{11} & C_{12} & C_{16} \\ C_{12} & C_{22} & C_{26} \\ C_{16} & C_{26} & C_{66} \end{bmatrix} \qquad \mathbf{C}_{pn}^k = \begin{bmatrix} 0 & 0 & C_{13} \\ 0 & 0 & C_{23} \\ 0 & 0 & C_{36} \end{bmatrix}$$

$$\mathbf{C}_{np}^k = \begin{bmatrix} 0 & 0 & 0 \\ 0 & 0 & 0 \\ C_{13} & C_{23} & C_{36} \end{bmatrix} \qquad \mathbf{C}_{nn}^k = \begin{bmatrix} C_{55} & C_{45} & 0 \\ C_{45} & C_{44} & 0 \\ 0 & 0 & C_{33} \end{bmatrix}$$

$$(5)$$

The three displacement components u_x, u_y and u_z and their relative variations can be modelled as:

$$(u_x, u_y, u_z) = F_\tau \left(u_{x\tau}, u_{y\tau}, u_{z\tau} \right) \qquad (\delta u_x, \delta u_y, \delta u_z) = F_s \left(\delta u_{xs}, \delta u_{ys}, \delta u_{zs} \right) \quad (6)$$

with Taylor expansions from first up to 4th order: $F_0 = z^0 = 1$, $F_1 = z^1 = z$, ..., $F_N = z^N$, ..., $F_4 = z^4$ if an Equivalent Single Layer (ESL) approach is used.

In case of Layer Wise (LW) models, each layer k of the given multi-layered structure is separately considered:

$$(u_x^k, u_y^k, u_z^k) = F_\tau^k \left(u_{x\tau}^k, u_{y\tau}^k, u_{z\tau}^k \right) \qquad (\delta u_x^k, \delta u_y^k, \delta u_z^k) = F_s^k \left(\delta u_{xs}^k, \delta u_{ys}^k, \delta u_{zs}^k \right)$$

$$(7)$$

where combinations of Legendre polynomials are employed as thickness functions:

$$F_t = \frac{P_0 + P_1}{2} \qquad F_b = \frac{P_0 - P_1}{2} \qquad F_l = P_l - P_{l-2}$$

$$\text{with} \quad \tau, s = t, b, l \quad \text{and} \quad l = 2, \dots, 14 \quad (8)$$

Here, t and b indicate the top and bottom values for each layer, P_l are the Legendre polynomials ($P_0 = 1$, $P_1 = \zeta_k$, $P_2 = \frac{(3\zeta_k^2 - 1)}{2}$ and so on) with $\zeta_k = \frac{2z^k}{h^k}$ that is the non-dimensionalized thickness coordinate ranging from -1 to $+1$ in each layer k. z_k is the local coordinate and h_k is the thickness of the kth layer.
The chosen functions have the following interesting properties:

$$\zeta_k = +1: \quad F_t = 1; \quad F_b = 0; \quad F_l = 0 \qquad \text{at the top}$$

$$\zeta_k = -1: \quad F_t = 0; \quad F_b = 1; \quad F_l = 0 \qquad \text{at the bottom}$$

$$(9)$$

4

It is obvious that for a single layer shell the ESL and LW evaluations coincide.

In the present formulation, we choose

$$F_t^k = [\frac{1 - 2/h_k \left(z - \frac{1}{2}\left(z_k + z_{k+1}\right)\right)}{2} \quad \frac{1 + 2/h_k \left(z - \frac{1}{2}\left(z_k + z_{k+1}\right)\right)}{2}]$$

for displacements u, v, w. Note that z_k, z_{k+1} correspond to the bottom and top z-coordinates for each layer k. We then obtain all terms of the equations of motion by integrating through the thickness direction.

It is interesting to note that under this combination of the Unified Formulation and RBF collocation, the collocation code depends only on the choice of F_t, F_s, in order to solve this type of problems. We designed a MATLAB code that just by changing F_t, F_s can analyse static deformations and free vibrations for any type of C° shear deformation theory.

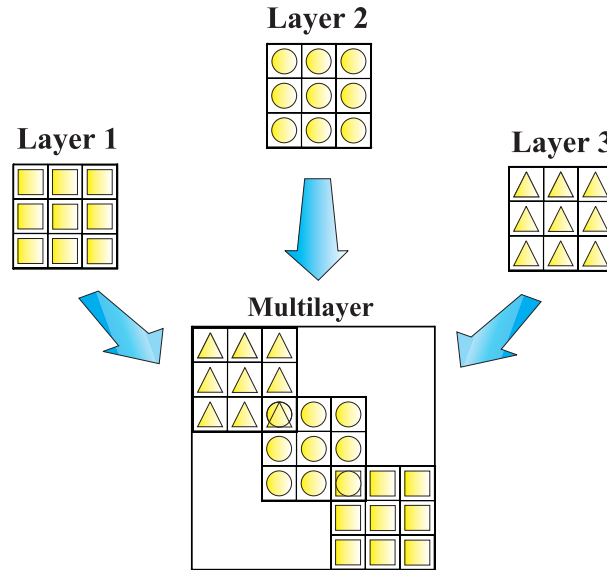In figure 2 it is shown the assembling procedures on layer k for LW approach.

Fig. 2. Assembling procedure for LW approach.

Substituting the geometrical relations, the constitutive equations and the unified formulation into the variational statement PVD, for the kth layer, one

has:

$$\int\limits_{\Omega_k}\int\limits_{A_k}\Big[(\mathbf{D}_p^k\ F_s\delta\mathbf{u}_s^k)^T(\mathbf{C}_{pp}^k\mathbf{D}_p^k\ F_\tau\mathbf{u}_\tau^k+\mathbf{C}_{pn}^k(\mathbf{D}_{n\Omega}^k+\mathbf{D}_{nz}^k)F_\tau\mathbf{u}_\tau^k)$$
$$+((\mathbf{D}_{n\Omega}^k+\mathbf{D}_{nz}^k)F_s\delta\mathbf{u}_s^k)^T(\mathbf{C}_{np}^k\mathbf{D}_p^k\ F_\tau\mathbf{u}_\tau^k+\mathbf{C}_{nn}^k(\mathbf{D}_{n\Omega}^k+\mathbf{D}_{nz}^k)F_\tau\mathbf{u}_\tau^k)\Big]d\Omega_kdz=\delta L_e^k \tag{10}$$

At this point, the formula of integration by parts is applied:

$$\int_{\Omega_k}\left((\mathbf{D}_\Omega)\delta\mathbf{a}^k\right)^T\mathbf{a}^kd\Omega_k=-\int_{\Omega_k}\delta\mathbf{a}^{kT}\left((\mathbf{D}_\Omega^T)\mathbf{a}^k\right)d\Omega_k+\int_{\Gamma_k}\delta\mathbf{a}^{kT}\left((\mathbf{I}_\Omega)\mathbf{a}^k\right)d\Gamma_k \tag{11}$$

where $\mathbf{I}_\Omega$ matrix is obtained applying the *Gradient theorem*:

$$\int_\Omega\frac{\partial\psi}{\partial x_i}dv=\oint_\Gamma n_i\psi ds \tag{12}$$

being n_i the components of the normal $\hat{n}$ to the boundary along the direction i. After integration by parts, the governing equations and boundary conditions for the plate in the mechanical case are obtained:

$$\int\limits_{\Omega_k}\int\limits_{A_k}(\ \delta\mathbf{u}_s^k)^T\Big[\Big((-\mathbf{D}_p^k)^T\Big(\mathbf{C}_{pp}^k(\mathbf{D}_p^k)\ +\mathbf{C}_{pn}^k(\mathbf{D}_{n\Omega}^k+\mathbf{D}_{nz}^k)$$
$$+\Big(-\mathbf{D}_{n\Omega}^k+\mathbf{D}_{nz}^k\Big)^T\Big(\mathbf{C}_{np}^k(\mathbf{D}_p^k)+\mathbf{C}_{nn}^k(\mathbf{D}_{n\Omega}^k+\mathbf{D}_{nz}^k)\Big)\Big)\mathbf{F}_\tau\mathbf{F}_s\mathbf{u}_\tau^k\Big]dxdydz$$
$$+\int\limits_{\Omega_k}\int\limits_{A_k}(\ \delta\mathbf{u}_s^k)^T\Big[\Big(\mathbf{I}_p^{kT}\Big(\mathbf{C}_{pp}^k(\mathbf{D}_p^k)\ +\mathbf{C}_{pn}^k(\mathbf{D}_{n\Omega}^k+\mathbf{D}_{nz}^k)\Big)$$
$$+\mathbf{I}_{np}^{kT}\Big(\mathbf{C}_{np}^k(\mathbf{D}_p^k)\ +\mathbf{C}_{nn}^k(\mathbf{D}_{n\Omega}^k+\mathbf{D}_{nz}^k)\Big)\Big)\mathbf{F}_\tau\mathbf{F}_s\mathbf{u}_\tau^k\Big]dxdydz=\int_{\Omega_k}\delta\mathbf{u}_s^{kT}F_s\mathbf{p}_u^kd\Omega_k\ . \tag{13}$$

where $\mathbf{I}_p^k$ and $\mathbf{I}_{np}^k$ depend on the boundary geometry:

$$\mathbf{I}_p^k=\begin{bmatrix}n_x&0&0\\0&n_y&0\\n_y&n_x&0\end{bmatrix}\ ,\quad\mathbf{I}_{np}^k=\begin{bmatrix}0&0&n_x\\0&0&n_y\\0&0&0\end{bmatrix}\ . \tag{14}$$

6

The normal to the boundary of domain Ω is:

$$\widehat{\mathbf{n}} = \begin{bmatrix} n_x \\ n_y \end{bmatrix} = \begin{bmatrix} cos(\varphi_x) \\ cos(\varphi_y) \end{bmatrix} \tag{15}$$

where φ_x and φ_y are the angles between the normal $\widehat{n}$ and the direction x and y respectively.

The governing equations for a multi-layered plate subjected to mechanical loadings are:

$$\delta \mathbf{u}_s^{kT} : \qquad \mathbf{K}_{uu}^{k\tau s}\, \mathbf{u}_\tau^k \; = \; \mathbf{P}_{u\tau}^k \tag{16}$$

where the fundamental nucleus $\mathbf{K}_{uu}^{k\tau s}$ is obtained as:

$$\mathbf{K}_{uu}^{k\tau s} = \Big[\big(-\mathbf{D}_p^k \big)^T \big(\mathbf{C}_{pp}^k (\mathbf{D}_p^k) \; + \mathbf{C}_{pn}^k (\mathbf{D}_{n\Omega}^k + \mathbf{D}_{nz}^k) \big) \\ + \big(-\mathbf{D}_{n\Omega}^k + \mathbf{D}_{nz}^k \big)^T \big(\mathbf{C}_{np}^k (\mathbf{D}_p^k) + \mathbf{C}_{nn}^k (\mathbf{D}_{n\Omega}^k + \mathbf{D}_{nz}^k) \big) \Big] \mathbf{F}_\tau \mathbf{F}_s \tag{17}$$

and the corresponding Neumann-type boundary conditions on Γ_k are:

$$\boldsymbol{\Pi}_d^{k\tau s}\, \mathbf{u}_\tau^k \; = \; \boldsymbol{\Pi}_d^{k\tau s}\, \bar{\mathbf{u}}_\tau^k \;, \tag{18}$$

where:

$$\boldsymbol{\Pi}_d^{k\tau s} = \Big[\mathbf{I}_p^{kT} \big(\mathbf{C}_{pp}^k (\mathbf{D}_p^k) \; + \mathbf{C}_{pn}^k (\mathbf{D}_{n\Omega}^k + \mathbf{D}_{nz}^k) \big) + \\ \mathbf{I}_{np}^{kT} \big(\mathbf{C}_{np}^k (\mathbf{D}_p^k) \; + \mathbf{C}_{nn}^k (\mathbf{D}_{n\Omega}^k + \mathbf{D}_{nz}^k) \big) \Big] \mathbf{F}_\tau \mathbf{F}_s \tag{19}$$

and $\mathbf{P}_{u\tau}^k$ are variationally consistent loads with applied pressure.

2.2 Fundamental nuclei

The fundamental nuclei in explicit form are then obtained as:

$$
\begin{aligned}
K_{uu_{11}}^{k\tau s} &= (-\partial_x^\tau \partial_x^s C_{11} - \partial_x^\tau \partial_y^s C_{16} + \partial_z^\tau \partial_z^s C_{55} - \partial_y^\tau \partial_x^s C_{16} - \partial_y^\tau \partial_y^s C_{66}) F_\tau F_s \\
K_{uu_{12}}^{k\tau s} &= (-\partial_x^\tau \partial_y^s C_{12} - \partial_x^\tau \partial_x^s C_{16} + \partial_z^\tau \partial_z^s C_{45} - \partial_y^\tau \partial_y^s C_{26} - \partial_y^\tau \partial_x^s C_{66}) F_\tau F_s \\
K_{uu_{13}}^{k\tau s} &= (-\partial_x^\tau \partial_z^s C_{13} - \partial_y^\tau \partial_z^s C_{36} + \partial_z^\tau \partial_y^s C_{45} + \partial_z^\tau \partial_x^s C_{55}) F_\tau F_s \\
K_{uu_{21}}^{k\tau s} &= (-\partial_y^\tau \partial_x^s C_{12} - \partial_y^\tau \partial_y^s C_{26} + \partial_z^\tau \partial_z^s C_{45} - \partial_x^\tau \partial_x^s C_{16} - \partial_x^\tau \partial_y^s C_{66}) F_\tau F_s \\
K_{uu_{22}}^{k\tau s} &= (-\partial_y^\tau \partial_y^s C_{22} - \partial_y^\tau \partial_x^s C_{26} + \partial_z^\tau \partial_z^s C_{44} - \partial_x^\tau \partial_y^s C_{26} - \partial_x^\tau \partial_x^s C_{66}) F_\tau F_s \quad (20) \\
K_{uu_{23}}^{k\tau s} &= (-\partial_y^\tau \partial_z^s C_{23} - \partial_x^\tau \partial_z^s C_{36} + \partial_z^\tau \partial_y^s C_{44} + \partial_z^\tau \partial_x^s C_{45}) F_\tau F_s \\
K_{uu_{31}}^{k\tau s} &= (\partial_z^\tau \partial_x^s C_{13} + \partial_z^\tau \partial_y^s C_{36} - \partial_y^\tau \partial_z^s C_{45} - \partial_x^\tau \partial_z^s C_{55}) F_\tau F_s \\
K_{uu_{32}}^{k\tau s} &= (\partial_z^\tau \partial_y^s C_{23} + \partial_z^\tau \partial_x^s C_{36} - \partial_y^\tau \partial_z^s C_{44} - \partial_x^\tau \partial_z^s C_{45}) F_\tau F_s \\
K_{uu_{33}}^{k\tau s} &= (\partial_z^\tau \partial_z^s C_{33} - \partial_y^\tau \partial_y^s C_{44} - \partial_y^\tau \partial_x^s C_{45} - \partial_x^\tau \partial_y^s C_{45} - \partial_x^\tau \partial_x^s C_{55}) F_\tau F_s
\end{aligned}
$$

$$
\begin{aligned}
\Pi_{11}^{k\tau s} &= (n_x \partial_x^s C_{11} + n_x \partial_y^s C_{16} + n_y \partial_x^s C_{16} + n_y \partial_y^s C_{66}) F_\tau F_s \\
\Pi_{12}^{k\tau s} &= (n_x \partial_y^s C_{12} + n_x \partial_x^s C_{16} + n_y \partial_y^s C_{26} + n_y \partial_x^s C_{66}) F_\tau F_s \\
\Pi_{13}^{k\tau s} &= (n_x \partial_z^s C_{13} + n_y \partial_z^s C_{36}) F_\tau F_s \\
\Pi_{21}^{k\tau s} &= (n_y \partial_x^s C_{12} + n_y \partial_y^s C_{26} + n_x \partial_x^s C_{16} + n_x \partial_y^s C_{66}) F_\tau F_s \\
\Pi_{22}^{k\tau s} &= (n_y \partial_y^s C_{22} + n_y \partial_x^s C_{26} + n_x \partial_y^s C_{26} + n_x \partial_x^s C_{66}) F_\tau F_s \quad (21) \\
\Pi_{23}^{k\tau s} &= (n_y \partial_z^s C_{23} + n_x \partial_z^s C_{36}) F_\tau F_s \\
\Pi_{31}^{k\tau s} &= (n_y \partial_z^s C_{45} + n_x \partial_z^s C_{55}) F_\tau F_s \\
\Pi_{32}^{k\tau s} &= (n_y \partial_z^s C_{44} + n_x \partial_z^s C_{45}) F_\tau F_s \\
\Pi_{33}^{k\tau s} &= (n_y \partial_y^s C_{44} + n_y \partial_x^s C_{45} + n_x \partial_y^s C_{45} + n_x \partial_x^s C_{55}) F_\tau F_s
\end{aligned}
$$

2.3 Dynamic governing equations

The PVD for the dynamic case is expressed as:

$$
\sum_{k=1}^{N_l} \int_{\Omega_k} \int_{A_k} \left\{ \delta \epsilon_{pG}^{k}{}^{T} \sigma_{pC}^k + \delta \epsilon_{nG}^{k}{}^{T} \sigma_{nC}^k \right\} d\Omega_k dz = \sum_{k=1}^{N_l} \int_{\Omega_k} \int_{A_k} \rho^k \delta \mathbf{u}^{kT} \ddot{\mathbf{u}}^k d\Omega_k dz + \sum_{k=1}^{N_l} \delta L_e^k
$$
$$(22)$$

where ρ^k is the mass density of the k-th layer and double dots denote acceleration.

By substituting the geometrical relations, the constitutive equations and the

Unified Formulation, we obtain the following governing equations:

$$\delta \mathbf{u}_s^{k^T} : \qquad \mathbf{K}_{uu}^{k\tau s}\, \mathbf{u}_\tau^k = \mathbf{M}^{k\tau s}\ddot{\mathbf{u}}_\tau^k + \mathbf{P}_{u\tau}^k \qquad (23)$$

In the case of free vibrations one has:

$$\delta \mathbf{u}_s^{k^T} : \qquad \mathbf{K}_{uu}^{k\tau s}\, \mathbf{u}_\tau^k = \mathbf{M}^{k\tau s}\ddot{\mathbf{u}}_\tau^k \qquad (24)$$

where $\mathbf{M}^{k\tau s}$ is the fundamental nucleus for the inertial term. The explicit form of that is:

$$
\begin{aligned}
M_{11}^{k\tau s} &= \rho^k F_\tau F_s; & M_{12}^{k\tau s} &= 0; & M_{13}^{k\tau s} &= 0 & (25) \\
M_{21}^{k\tau s} &= 0; & M_{22}^{k\tau s} &= \rho^k F_\tau F_s; & M_{23}^{k\tau s} &= 0 & (26) \\
M_{31}^{k\tau s} &= 0; & M_{32}^{k\tau s} &= 0; & M_{33}^{k\tau s} &= \rho^k F_\tau F_s & (27)
\end{aligned}
$$

The geometrical and mechanical boundary conditions are the same of the static case.

3   The radial basis function method

For the sake of completeness we present here the basics of collocation with radial basis functions for static and vibrations problems.

3.1   The static problem

In this section the formulation of a global unsymmetrical collocation RBF-based method to compute elliptic operators is presented. Consider a linear elliptic partial differential operator L and a bounded region Ω in $\mathbb{R}^n$ with some boundary $\partial\Omega$. In the static problems we seek the computation of displacements ($\mathbf{u}$) from the global system of equations

$$\mathcal{L}\mathbf{u} = \mathbf{f} \text{ in } \Omega \qquad (28)$$

$$\mathcal{L}_B\mathbf{u} = \mathbf{g} \text{ on } \partial\Omega \qquad (29)$$

where $\mathcal{L}$, $\mathcal{L}_B$ are linear operators in the domain and on the boundary, respectively. The right-hand side of (28) and (29) represent the external forces applied on the plate and the boundary conditions applied along the perimeter

of the plate, respectively. The PDE problem defined in (28) and (29) will be replaced by a finite problem, defined by an algebraic system of equations, after the radial basis expansions.

3.2 The eigenproblem

The eigenproblem looks for eigenvalues (λ) and eigenvectors ($\mathbf{u}$) that satisfy

$$\mathcal{L}\mathbf{u} + \lambda\mathbf{u} = 0 \text{ in } \Omega \tag{30}$$

$$\mathcal{L}_B\mathbf{u} = 0 \text{ on } \partial\Omega \tag{31}$$

As in the static problem, the eigenproblem defined in (30) and (31) is replaced by a finite-dimensional eigenvalue problem, based on RBF approximations.

3.3 Radial basis functions approximations

The radial basis function (ϕ) approximation of a function ($\mathbf{u}$) is given by

$$\widetilde{\mathbf{u}}(\mathbf{x}) = \sum_{i=1}^{N} \alpha_i \phi\left(\|x - y_i\|_2\right), \mathbf{x} \in \mathbb{R}^n \tag{32}$$

where $y_i, i = 1, .., N$ is a finite set of distinct points (centers) in $\mathbb{R}^n$. Although we can use many RBFs, in this paper we restrict to the Wendland function, defined as

$$\phi(r) = (1 - c\ r)_+^8 \left(32(c\ r)^3 + 25(c\ r)^2 + 8c\ r + 1\right) \tag{33}$$

where the Euclidian distance r is real and non-negative and c is a positive shape parameter. The shape parameter (c) was obtained by an optimization procedure, as detailed in Ferreira and Fasshauer [11].

Considering N distinct interpolations, and knowing $u(x_j), j = 1, 2, ..., N$, we find α_i by the solution of a $N \times N$ linear system

$$\mathbf{A}\boldsymbol{\alpha} = \mathbf{u} \tag{34}$$

where $\mathbf{A} = [\phi\left(\|x - y_i\|_2\right)]_{N \times N}$, $\boldsymbol{\alpha} = [\alpha_1, \alpha_2, ..., \alpha_N]^T$ and $\mathbf{u} = [u(x_1), u(x_2), ..., u(x_N)]^T$.

3.4 Solution of the static problem

The solution of a static problem by radial basis functions considers N_I nodes in the domain and N_B nodes on the boundary, with a total number of nodes $N = N_I + N_B$. We denote the sampling points by $x_i \in \Omega, i = 1, ..., N_I$ and $x_i \in \partial\Omega, i = N_I + 1, ..., N$. At the points in the domain we solve the following system of equations

$$\sum_{i=1}^{N} \alpha_i \mathcal{L}\phi \left(\|x - y_i\|_2 \right) = \mathbf{f}(x_j), j = 1, 2, ..., N_I \tag{35}$$

or

$$\mathcal{L}^I \boldsymbol{\alpha} = \mathbf{F} \tag{36}$$

where

$$\mathcal{L}^I = [\mathcal{L}\phi \left(\|x - y_i\|_2 \right)]_{N_I \times N} \tag{37}$$

At the points on the boundary, we impose boundary conditions as

$$\sum_{i=1}^{N} \alpha_i \mathcal{L}_B \phi \left(\|x - y_i\|_2 \right) = \mathbf{g}(x_j), j = N_I + 1, ..., N \tag{38}$$

or

$$\mathbf{B}\boldsymbol{\alpha} = \mathbf{G} \tag{39}$$

where

$$\mathbf{B} = \mathcal{L}_B \phi \left[(\|x_{N_I+1} - y_j\|_2) \right]_{N_B \times N}$$

Therefore, we can write a finite-dimensional static problem as

$$\begin{bmatrix} \mathcal{L}^I \\ \mathbf{B} \end{bmatrix} \boldsymbol{\alpha} = \begin{bmatrix} \mathbf{F} \\ \mathbf{G} \end{bmatrix} \tag{40}$$

By inverting the system (40), we obtain the vector $\boldsymbol{\alpha}$. We then obtain the solution $\mathbf{u}$ using the interpolation equation (32).

3.5 Solution of the eigenproblem

We consider N_I nodes in the interior of the domain and N_B nodes on the boundary, with $N = N_I + N_B$. We denote interpolation points by $x_i \in \Omega, i = 1, ..., N_I$ and $x_i \in \partial\Omega, i = N_I + 1, ..., N$. At the points in the domain, we define the eigenproblem as

$$\sum_{i=1}^{N} \alpha_i \mathcal{L}\phi \left(\|x - y_i\|_2 \right) = \lambda \tilde{\mathbf{u}}(x_j), j = 1, 2, ..., N_I \tag{41}$$

11

or

$$\mathcal{L}^I \boldsymbol{\alpha} = \lambda \tilde{\mathbf{u}}^I \qquad (42)$$

where

$$\mathcal{L}^I = [\mathcal{L}\phi\left(\|x - y_i\|_2\right)]_{N_I \times N} \qquad (43)$$

At the points on the boundary, we enforce the boundary conditions as

$$\sum_{i=1}^N \alpha_i \mathcal{L}_B \phi\left(\|x - y_i\|_2\right) = 0, j = N_I + 1, ..., N \qquad (44)$$

or

$$\mathbf{B}\boldsymbol{\alpha} = 0 \qquad (45)$$

Equations (42) and (45) can now be solved as a generalized eigenvalue problem

$$\begin{bmatrix} \mathcal{L}^I \\ \mathbf{B} \end{bmatrix} \boldsymbol{\alpha} = \lambda \begin{bmatrix} \mathbf{A}^I \\ \mathbf{0} \end{bmatrix} \boldsymbol{\alpha} \qquad (46)$$

where

$$\mathbf{A}^I = \phi\left[(\|x_{N_I} - y_j\|_2)\right]_{N_I \times N}$$

3.6 Discretization of the equations of motion and boundary conditions

The radial basis collocation method follows a simple implementation procedure. Taking equation (13), we compute

$$\boldsymbol{\alpha} = \begin{bmatrix} L^I \\ \mathbf{B} \end{bmatrix}^{-1} \begin{bmatrix} \mathbf{F} \\ \mathbf{G} \end{bmatrix} \qquad (47)$$

This $\boldsymbol{\alpha}$ vector is then used to obtain solution $\tilde{\mathbf{u}}$, by using (7). If derivatives of $\tilde{\mathbf{u}}$ are needed, such derivatives are computed as

$$\frac{\partial \tilde{\mathbf{u}}}{\partial x} = \sum_{j=1}^N \alpha_j \frac{\partial \phi_j}{\partial x} \qquad (48)$$

$$\frac{\partial^2 \tilde{\mathbf{u}}}{\partial x^2} = \sum_{j=1}^N \alpha_j \frac{\partial^2 \phi_j}{\partial x^2}, \text{etc} \qquad (49)$$

In the present collocation approach, we need to impose essential and natural boundary conditions. Consider, for example, the condition $w = 0$, on a simply

supported or clamped edge. We enforce the conditions by interpolating as

$$w = 0 \rightarrow \sum_{j=1}^{N} \alpha_j^W \phi_j = 0 \qquad (50)$$

Other boundary conditions are interpolated in a similar way.

3.7 Free vibrations problems

For free vibration problems we set the external force to zero, and assume harmonic solution in terms of displacements u^k, v^k, w^k, for each layer, as

$$u^k = U^k(w, y)e^{i\omega t}; \quad v^k = V^k(w, y)e^{i\omega t}; \quad w^k = W^k(w, y)e^{i\omega t} \qquad (51)$$

where ω is the frequency of natural vibration. Substituting the harmonic expansion into equations (46) in terms of the amplitudes U^k, V^k, W^k, we may obtain the natural frequencies and vibration modes for the plate problem, by solving the eigenproblem

$$\left[\mathcal{L} - \omega^2 \mathcal{G} \right] \mathbf{X} = \mathbf{0} \qquad (52)$$

where $\mathcal{L}$ collects all stiffness terms and $\mathcal{G}$ collects all terms related to the inertial terms. In (52) $\mathbf{X}$ are the modes of vibration associated with the natural frequencies defined as ω.

4 Numerical examples

All numerical examples consider a Chebyshev grid.

4.1 Static problems-cross-ply laminated plates

A simply supported square laminated plate of side a and thickness h is composed of four equally layers oriented at $[0°/90°/90°/0°]$. The plate is subjected to a sinusoidal vertical pressure of the form

$$p_z = P \sin\left(\frac{\pi x}{a}\right) \sin\left(\frac{\pi y}{a}\right)$$

13

with the origin of the coordinate system located at the lower left corner on the midplane and P the maximum load (at center of plate). Note that the load can now be applied at the top surface ($z = h/2$), or middle-surface ($z = 0$), because the formulation considers transverse displacements in every layer interface.

The orthotropic material properties for each layer are given by

$$E_1 = 25.0E_2 \qquad G_{12} = G_{13} = 0.5E_2 \qquad G_{23} = 0.2E_2 \qquad \nu_{12} = 0.25$$

The in-plane displacements, the transverse displacements, the normal stresses and the in-plane and transverse shear stresses are presented in normalized form as

$$\overline{w} = \frac{10^2 w_{(a/2,a/2,0)} h^3 E_2}{Pa^4} \qquad \overline{\sigma}_{xx} = \frac{\sigma_{xx(a/2,a/2,h/2)} h^2}{Pa^2} \qquad \overline{\sigma}_{yy} = \frac{\sigma_{yy(a/2,a/2,h/4)} h^2}{Pa^2}$$

$$\overline{\tau}_{xz} = \frac{\tau_{xz(0,a/2,0)} h}{Pa} \qquad \overline{\tau}_{xy} = \frac{\tau_{xy(0,0,h/2)} h^2}{Pa^2}$$

In Table 1 we present results for for the present layerwise theory, using 11×11 up to 17×17 points. We compare results with higher-order solutions by Akhras [12] , and Reddy [13], FSDT solutions by Reddy and Chao [14], and an exact solution by Pagano [15]. We also compare with results by the authors using RBFs with Reddy's theory [8], and a layerwise theory [16]. Our layerwise theory produces excellent results, when compared with other HSDT theories, for all a/h ratios, for transverse displacements, normal stresses and transverse shear stresses. In Figure 3 the σ_{xx} evolution across the thickness direction is illustrated, for $a/h = 4$, using 13×13 points, considering a top surface load. In Figure 4 the τ_{xz} evolution across the thickness direction is illustrated, for $a/h = 4$, using 13×13 points, considering a top surface load. In Figure 5 the σ_{xx} evolution across the thickness direction is illustrated, for $a/h = 4$, using 13×13 points, considering the load applied at the middle surface. In Figure 6 the τ_{xz} evolution across the thickness direction is illustrated, for $a/h = 4$, using 13×13 points, considering the load applied at the middle surface. The application of the load at the top surface brings the stress profiles to be unsymmetrical with respect to the middle surface. Note that the transverse shear stresses are obtained directly from the constitutive equations.

$\frac{a}{h}$	Method	$\overline{w}$	$\overline{\sigma}_{xx}$	$\overline{\tau}_{zx}$
4	HSDT [13]	1.8937	0.6651	0.2064
	FSDT [14]	1.7100	0.4059	0.1398
	elasticity [15]	1.954	0.720	0.270
	present (11 × 11 grid)	1.9432	0.6494	0.2190
	present (13 × 13 grid)	1.9432	0.6497	0.2190
	present (17 × 17 grid)	1.9433	0.6497	0.2190
10	HSDT [13]	0.7147	0.5456	0.2640
	FSDT [14]	0.6628	0.4989	0.1667
	elasticity [15]	0.743	0.559	0.301
	present (11 × 11 grid)	0.7334	0.5548	0.3000
	present (13 × 13 grid)	0.7335	0.5549	0.2999
	present (17 × 17 grid)	0.7335	0.5550	0.2999
100	HSDT [13]	0.4343	0.5387	0.2897
	FSDT [14]	0.4337	0.5382	0.1780
	elasticity [15]	0.4347	0.539	0.339
	present (11 × 11 grid)	0.4339	0.5432	0.3336
	present (13 × 13 grid)	0.4351	0.5434	0.3358
	present (17 × 17 grid)	0.4353	0.5438	0.3361

Table 1
$[0°/90°/90°/0°]$ square laminated plate under layerwise formulation

4.2   Free vibration problems-cross-ply laminated plates

In this example, all layers of the laminate are assumed to be of the same thickness, density and made of the same linearly elastic composite material. The following material parameters of a layer are used:

$$\frac{E_1}{E_2} = 10, 20, 30 \text{ or } 40; G_{12} = G_{13} = 0.6E_2; G_3 = 0.5E_2; \nu_{12} = 0.25$$

The subscripts 1 and 2 denote the directions normal and transverse to the fiber direction in a lamina, which may be oriented at an angle to the plate axes. The ply angle of each layer is measured from the global x-axis to the fiber direction.
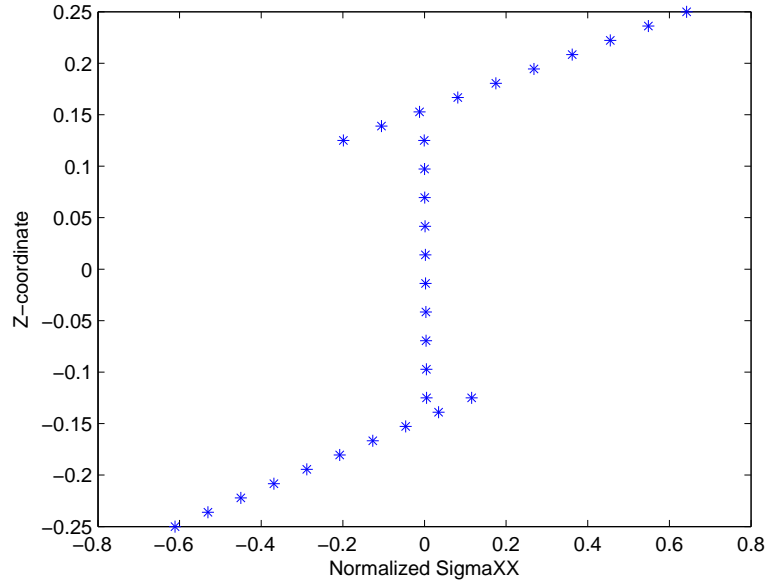
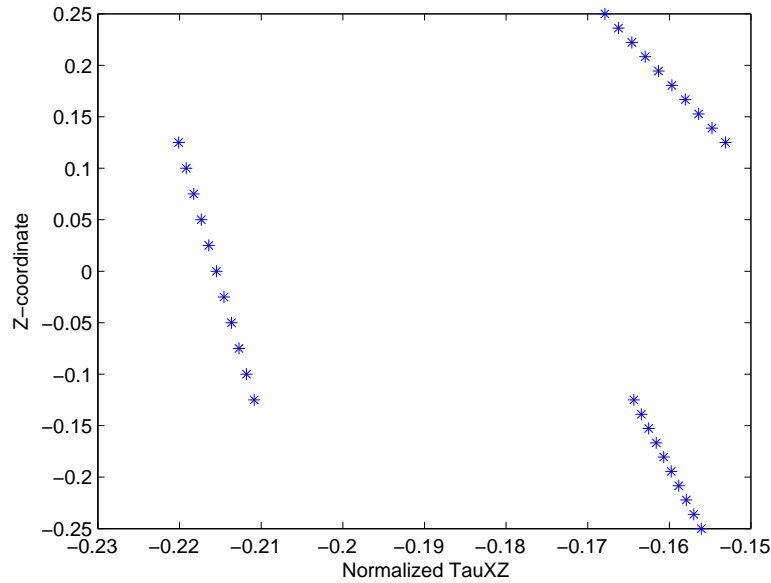Fig. 3. Normalized normal σ_{xx} stress for $a/h = 4$, 13×13 points, load at $z = h/2$

Fig. 4. Normalized transverse τ_{xz} stress for $a/h = 4$, 13×13 points, load at $z = h/2$

The example considered is a simply supported square plate of the cross-ply lamination $[0°/90°/90°/0°]$. The thickness and length of the plate are denoted by h and a, respectively. The thickness-to-span ratio $h/a = 0.2$ is employed in the computation. Table 2 lists the fundamental frequency of the simply supported laminate made of various modulus ratios of E_1/E_2. It is found that the present meshless results are in very close agreement with the values of [17,18] and the meshfree results of Liew [19] based on the FSDT. The
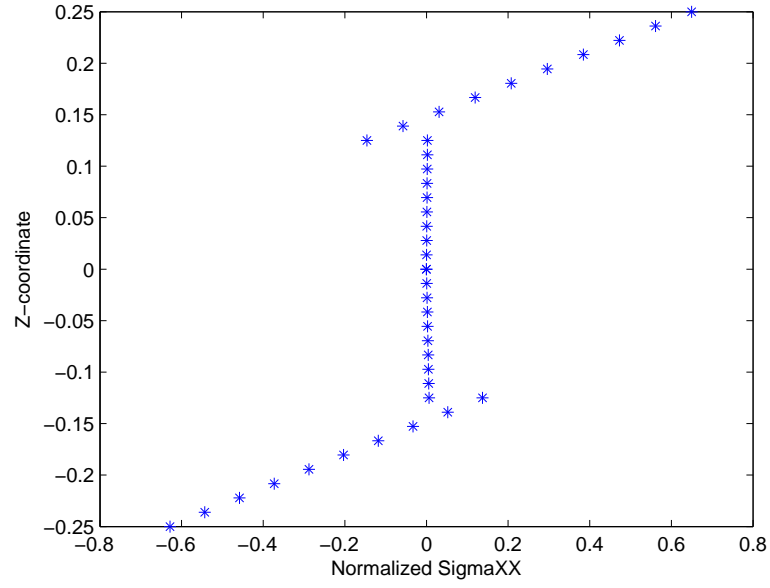
16

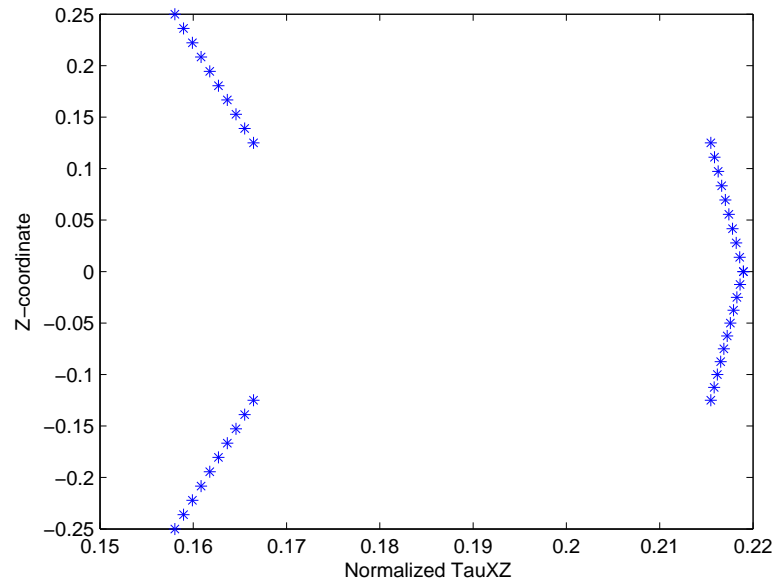Fig. 5. Normalized normal σ_{xx} stress for $a/h = 4$, 13×13 points, load at $z = 0$

Fig. 6. Normalized transverse τ_{xz} stress for $a/h = 4$, 13×13 points, load at $z = 0$

small differences may be due to the consideration of the through-the-thickness deformations in the present formulation.

4.3 Sandwich plate

In this example, we consider a simply-supported square sandwich plate loaded by uniform transverse pressure p. The length and thickness of the plate are denoted by a, h, respectively. The plate ratio a/h is taken as 10. It consists of a two skins with equal thickness ($0.1h$) with the following mechanical properties:

$$E_1/E_2 = 25; \quad G_{12}/E_2 = G_{13}/E_2 = 0.5; \quad G_{23}/E_2 = 0.2; \quad \nu_{12} = 0.25 \quad (53)$$

while the inner layer, the weak core, has a thickness of $0.8h$ and the following mechanical properties:

$$E_1/E_2 = 1; \quad G_{13}/E_2 = G_{23}/E_2 = 0.06; \quad G_{12}/E_2 = 0.016; \quad \nu_{12} = 0.25 \tag{54}$$

In Table 3 the present RBF formulation is compared with closed-form results by Carrera and Ciuffreda [20] [1].

Results are presented for transverse displacements $U_z(a/2, b/2, 0)$, and in-plane $S_{xx}(a/2, b/2, h/2)$ and out-of-plane stress $S_{xz}(0, b/2, 0)$. Figures 7, 9, 11 illustrate the evolution of the normal stress S_{xx} across the thickness direction, for $a/h = 4, 10, 100$, respectively. Figures 8, 10, 12 illustrate the evolution of the transverse shear stress S_{xz} across the thickness direction, for $a/h = 4, 10, 100$, respectively.

---

[1] Depending on the used variational statement (PVD or RMVT), the description of the variables (LWM or ESLM), the order of the used expansion N, a number of two-dimensional theories can be constructed. In order to denote different theories in a concise manner, acronims could conveniently used. Transverse stress and displacement z-fields have the assumptions for layer-wise mixed cases: LM1(Layerwise Mixed, linear) and LM4 (Layer-wise Mixed, fourth-order). Only displacement assumptions are made for LD1 (Layer-wise Displacement, linear) and LD3 (Layerwise Displacement, cubic) cases. A parabolic transverse stress field in each-layer is associated to linear a zig-zag diplacement field for the EMZC1 case (Equivalent-single-layer Mixed including Zig-zag and interlaminar-Continuity, linear) and fourth-order transverse stress field in each-layer is associated to a cubic zig-zag displacement field for the EMZC3 case (Equivalent-single-layer Mixed including Zig-zag and interlaminar-Continuity, cubic). The EMZC3d approach is related with a theory that accounts for constant W across the thickness direction ($w = w_0$). The ED4 and ED1 are Equivalent-single-layer displacement-based theories of the fourth-order and first-order types.
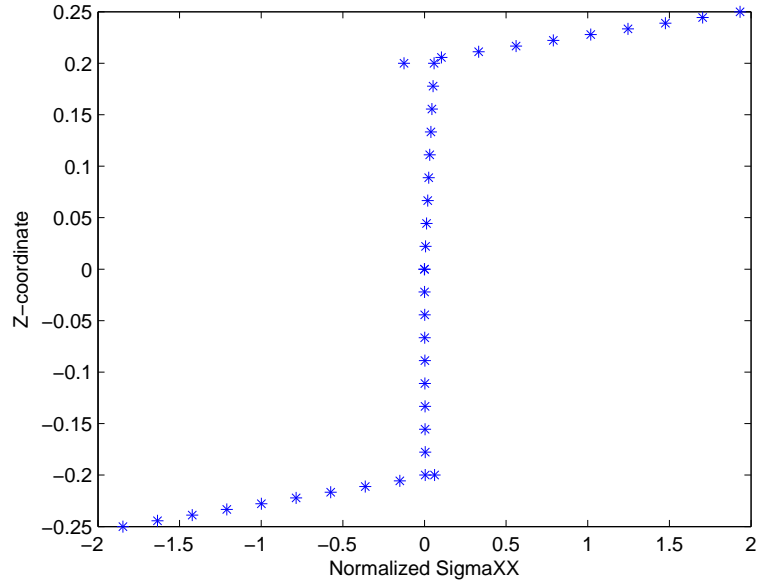
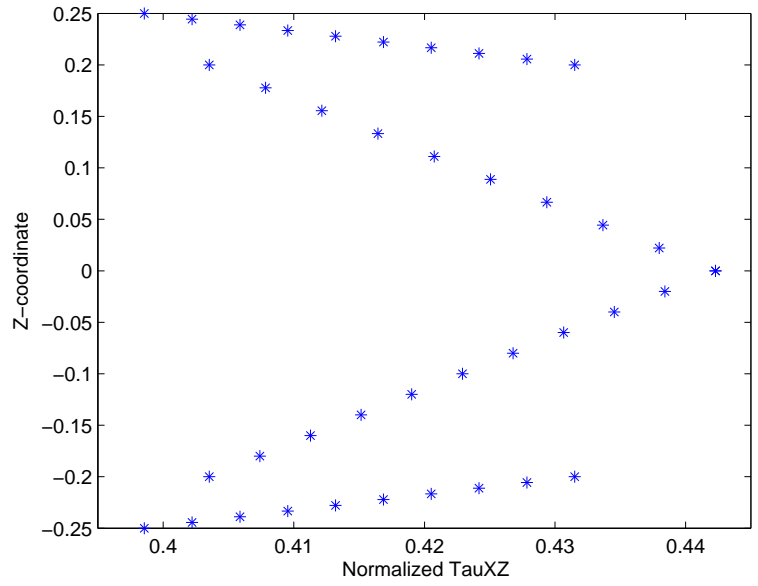Fig. 7. Normalized normal S_{xx} stress for $a/h = 4$, 13×13 points, load at $z = 0$

Fig. 8. Normalized transverse S_{xz} stress for $a/h = 4$, 13×13 points, load at $z = 0$

5 Conclusions

In this paper we presented a study using the radial basis function collocation method to analyse static deformations and free vibrations of thin and thick laminated and sandwich plates using a layerwise formulation, allowing for through-the-thickness deformations.This has not been done before and serves
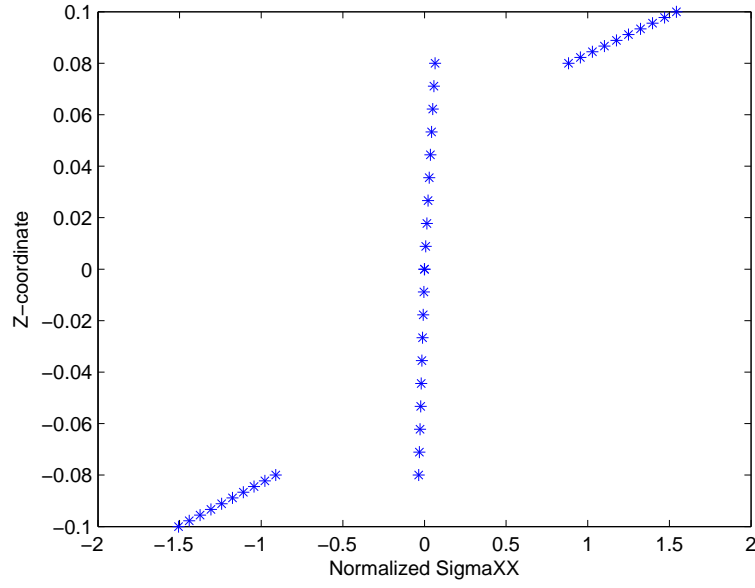
19

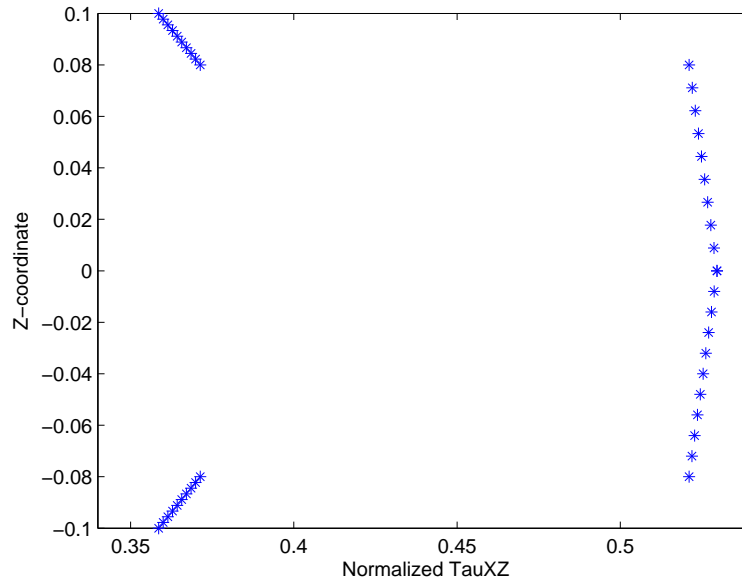Fig. 9. Normalized normal S_{xx} stress for $a/h = 10$, 13×13 points, load at $z = 0$

Fig. 10. Normalized transverse S_{xz} stress for $a/h = 10$, 13×13 points, load at $z = 0$

to fills the gap of knowledge in this area.

Using the Unified Formulation with the radial basis collocation, all the C^o plate formulations can be easily discretized by radial basis functions collocation. Also, the burden of deriving the equations of motion and boundary conditions is eliminated with the present approach. All is needed is to change one vector F_t that defines the expansion of displacements.
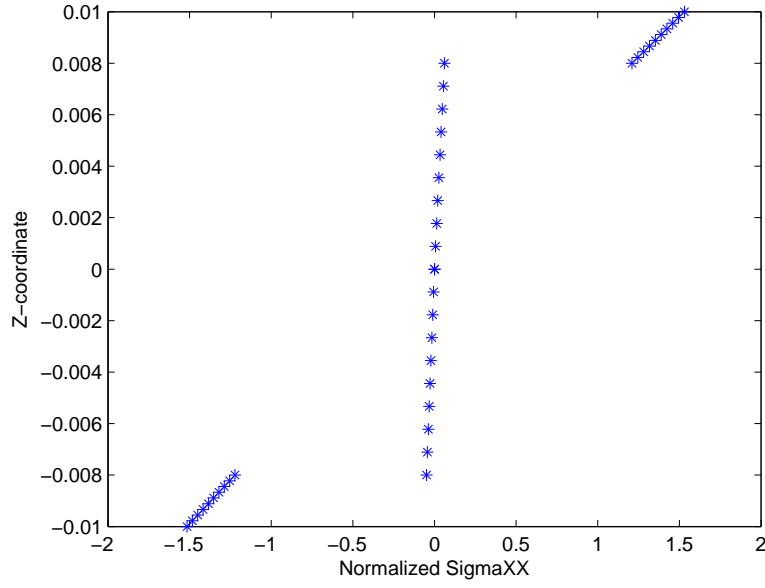
20

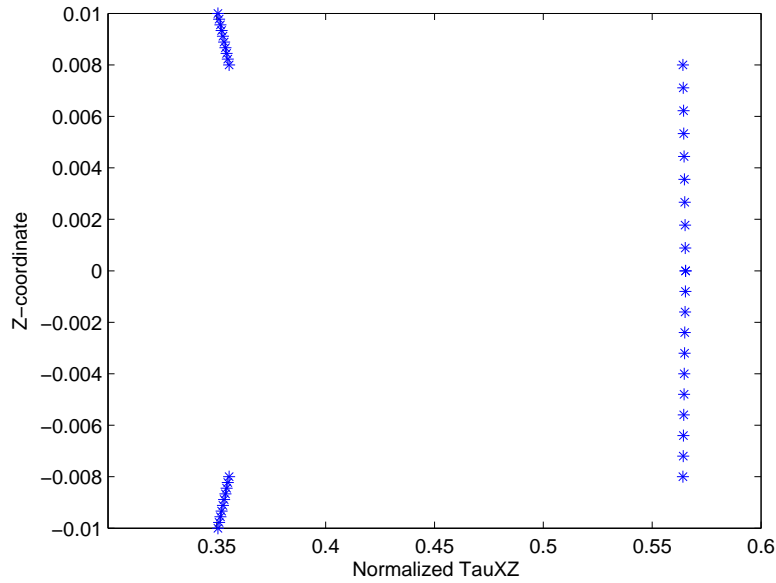Fig. 11. Normalized normal σ_{xx} stress for $a/h = 100$, 17×17 points, load at $z = 0$

Fig. 12. Normalized transverse τ_{xz} stress for $a/h = 100$, 17×17 points, load at $z = 0$

We analysed square cross-ply laminated plates in bending and free vibrations. The present results were compared with existing analytical solutions or competitive finite element solutions and excellent agreement was observed in all cases.

The present method is a simple yet powerful alternative to other finite element or meshless methods in the static deformation and free vibration analysis of

21

thin and thick isotropic or laminated or sandwich plates.

Acknowledgement

References

[1] E. Carrera. Historical review of zig-zag theories for multilayered plates and shells. *Applied Mechanics Reviews*, (56):287–308, 2003.

[2] G. Kirchhoff. Uber das gleichgewicht und die bewegung einer elastischen scheibe. *J. Angew. Math.*, 40:51–88, 1850.

[3] E. Reissner. The effect of transverse shear deformations on the bending of elastic plates. *Journal of Applied mechanics*, 12:A69–A77, 1945.

[4] R. D. Mindlin. Influence of rotary inertia and shear in flexural motions of isotropic elastic plates. *Journal of Applied mechanics*, 18:31–38, 1951.

[5] E. J. Kansa. Multiquadrics- a scattered data approximation scheme with applications to computational fluid dynamics. i: Surface approximations and partial derivative estimates. *Computers and Mathematics with Applications*, 19(8/9):127–145, 1990.

[6] A. J. M. Ferreira. A formulation of the multiquadric radial basis function method for the analysis of laminated composite plates. *Composite Structures*, 59:385–392, 2003.

[7] A. J. M. Ferreira. Thick composite beam analysis using a global meshless approximation based on radial basis functions. *Mechanics of Advanced Materials and Structures*, 10:271–284, 2003.

[8] A. J. M. Ferreira, C. M. C. Roque, and P. A. L. S. Martins. Analysis of composite plates using higher-order shear deformation theory and a finite point formulation based on the multiquadric radial basis function method. *Composites: Part B*, 34:627–636, 2003.

[9] E. Carrera. C^0 reissner-mindlin multilayered plate elements including zig-zag and interlaminar stress continuity. *International Journal of Numerical Methods in Engineering*, 39:1797–1820, 1996.

[10] E. Carrera. Developments, ideas, and evaluations based upon reissner's mixed variational theorem in the modelling of multilayered plates and shells. *Applied Mechanics Reviews*, 54:301–329, 2001.

[11] A. J. M. Ferreira and G. E. Fasshauer. Computation of natural frequencies of shear deformable beams and plates by a rbf-pseudospectral method. *Computer Methods in Applied Mechanics and Engineering*, 196:134–146, 2006.

[12] G. Akhras, M. S. Cheung, and W. Li. Finite strip analysis for anisotropic laminated composite plates using higher-order deformation theory. *Computers & Structures*, 52(3):471–477, 1994.

[13] J. N. Reddy. A simple higher-order theory for laminated composite plates. *Journal of Applied Mechanics*, 51:745–752, 1984.

[14] J. N. Reddy and W. C. Chao. A comparison of closed-form and finite-element solutions of thick laminated anisotropic rectangular plates. *Nuclear Engineering and Design*, 64:153–167, 1981.

[15] N. J. Pagano. Exact solutions for rectangular bidirectional composites and sandwich plates. *Journal of Composite Materials*, 4:20–34, 1970.

[16] A. J. M. Ferreira. Analysis of composite plates using a layerwise deformation theory and multiquadrics discretization. *Mechanics of Advanced Materials and Structures*, 12(2):99–112, 2005.

[17] J. N. Reddy. Bending of laminated anisotropic shells by a shear deformable finite element. *Fibre Science and Technology*, 17:9–24, 1982.

[18] A. A. Khdeir and L. Librescu. Analysis of symmetric cross-ply elastic plates using a higher-order theory,part ii: buckling and free vibration. *Composite Structures*, 9:259–277, 1988.

[19] K. M. Liew, Y. Q. Huang, and J. N. Reddy. Vibration analysis of symmetrically laminated plates based on fsdt using the moving least squares differential quadrature method. *Computer Methods in Applied Mechanics and Engineering*, 192:2203–2222, 2003.

[20] E. Carrera and A. Ciuffreda. A unified formulation to assess theories of multilayered plates for various bending problems. *Compos. Struct.*, 69:4271–293, 2005.

Method	Grid	E_1/E_2			
		10	20	30	40
Liew [19]		8.2924	9.5613	10.320	10.849
Exact (Reddy, Khdeir)[17,18]		8.2982	9.5671	10.326	10.854
Present layerwise ($\nu_{23} = 0.25$)	11×11	8.3435	9.6221	10.3738	10.8854
	13×13	8.3431	9.6218	10.3735	10.8850
	17×17	8.3430	9.6216	10.3733	10.8849

Table 2

The normalized fundamental frequency of the simply-supported cross-ply laminated square plate $[0°/90°/90°/0°]$ $(\bar{w} = (wa^2/h)\sqrt{\rho/E_2}, h/a = 0.2)$

	U_z			S_{xx}			S_{xz}		
a/h	4	10	100	4	10	100	4	10	100
11×11	10.8989	3.1330	1.2402	1.9940	1.5645	1.4923	0.4335	0.5248	0.5616
13×13	10.8857	3.1245	1.2757	1.9328	1.5437	1.5314	0.4423	0.5186	0.5654
17×17	10.893	3.1282	1.2748	1.9486	1.5503	1.5308	0.4489	0.5337	0.5743
LM4	10.682	3.083	1.262	1.902	1.509	1.505	0.4074	0.5276	0.5889
EMZC3	10.678	3.082	1.262	1.899	1.507	1.504	0.3949	0.5239	0.5886
EMZC3d	10.626	3.026	1.230	1.915	1.480	1.476	0.4031	0.5224	0.5865
ED4	9.909	2.923	1.260	1.929	1.519	1.506	0.3574	0.5104	0.5881
ED1	5.542	1.982	1.218	1.145	1.388	1.475	0.5249	0.5716	0.5876
FSDT	5.636	1.984	1.218	1.168	1.391	1.476	0.5249	0.5716	0.5876
CLT	1.2103	1.2103	1.2103	1.476	1.476	1.476	0.5878	0.5878	0.5878

Table 3

Load applied at $z = 0$: square sandwich plates